

Supplementary Information

Defect Engineering of VN Nanowires Enables Dual-Mode SERS-Colorimetric Quantification of Glutathione in Serum

Yao Liu^a, Chao Yang^a, Fei Li,^a Shan Liang^{a,}, Xianyin Song^c, Yawei Lv^{b,*}, Xingang Zhang^{a,*}, Changzhong Jiang^c*

^aKey Laboratory of Low-Dimensional Quantum Structures and Quantum Control of Ministry of Education, Key Laboratory for Matter Microstructure and Function of Hunan Province, Department of Physics and Synergetic Innovation Center for Quantum Effects and Applications, School of Physics and Electronics, Hunan Normal University, Changsha 410081, China

^bSchool of Physics and Electronics, Hunan University, Changsha 410082, China

^cCollege of Materials Science and Engineering, Hunan University, Changsha 410082, China

E-mail: zxcg@hunnu.edu.cn; liangshan@hunnu.edu.cn; lvyawei@hnu.edu.cn

Experimental Section

Synthesis of V-MOF Nanowires

The synthesis involved dissolving VCl_3 (0.025 g) and terephthalic acid (0.026 g) in 40 mL deionized water under 30 min magnetic stirring at room temperature. After CTAB addition, the solution underwent hydrothermal treatment in a Teflon-lined autoclave (200 °C, 48 h). The resulting product was purified through sequential washing with deionized water and anhydrous ethanol to obtain V-MOF nanowires.

Synthesis of VN@C Nanowires

The thermal treatment involved loading 0.03 g V-MOF nanowires into an alumina crucible within a controlled atmosphere furnace. After 30 min Ar purging, pyrolysis was conducted under flowing NH_3 (0.4 L min^{-1}) with a 5 °C min^{-1} to 500 °C (4 h dwell). Post-annealing cooling under Ar yielded a black product, subsequently purified through sequential deionized water/ethanol washing cycles and ambient drying.

Synthesis of P-VN@C Nanowires

The precursors (VN@C nanowires and NaH_2PO_2 in 1:3 mass ratio) were spatially separated in an alumina boat. Following 30 minutes Ar purging, thermal treatment was conducted with a 2 °C min^{-1} ramp to 300 °C (2 h dwell), followed by ambient cooling under Ar protection.

Synthesis of V_2O_5 Nanowires

The precursor solution was prepared by dispersing V_2O_5 (0.36 g) in deionized water (30 mL) with subsequent addition of 30% H_2O_2 (10 mL) under 2 hours magnetic stirring at ambient temperature. The homogeneous mixture underwent hydrothermal crystallization in a PTFE-lined autoclave at 200°C for 96 h. Post-synthesis processing included six-cycle deionized water washing and lyophilization to obtain V_2O_5 nanowires.

Peroxidase-like Activity of P-VN@C

The peroxidase-like activity of P-VN@C was monitored by SERS. A mixture of TMB solution (200 μL , 1 mM), H_2O_2 (200 μL , 1 mM), and P-VN@C dispersion (100 μL , 0.5 mg mL^{-1}) was prepared in acetate buffer (1.5 mL, pH = 4). After reacting at 37°C for 5 minutes, the oxidation of TMB was assessed by measuring the 1623 cm^{-1} peak intensity in the SERS spectrum.

The peroxidase-like activity of P-VN@C was demonstrated by the accelerated oxidation of TMB from colorless to blue in the presence of H_2O_2 , accompanied by an absorbance peak. In a 5 mL centrifuge tube, 100 μL of 0.5 mg/mL P-VN@C, 200 μL of 1 mM TMB solution, 200 μL of 1 mM H_2O_2 , and 1.5 mL of pH 4.0 acetate buffer were sequentially added and incubated at 37°C for 5 minutes. The POD-like activity was then assessed using UV-Vis spectroscopy. A control experiment was performed by mixing P-VN@C or H_2O_2 with TMB, and the UV absorbance spectra were collected for comparison.

Aqueous Glutathione Detection

The reaction system was constructed by sequentially loading 100 μL of 0.5 mg mL^{-1} P-VN@C dispersion, 200 μL each of 1 mM TMB and H_2O_2 solutions, along with freshly prepared GSH solutions (variable concentrations) into a 5 mL centrifuge tube.

The mixture was buffered with 1.5 mL acetate buffer (pH 4.0) to achieve total 2 mL system volume. Following 60 minutes incubation at 37 °C, spectrophotometric analyses including UV-Vis absorption and SERS were conducted to characterize optical responses.

Serum Glutathione Detection

Serum samples were donated by healthy volunteers from the Affiliated Hospital of Hunan Normal University, with informed consent obtained from all participants prior to collection. This study was approved by the Hunan Normal University Biomedical Research Ethics Committee (Reference No.2025-451). Blood samples were diluted 1,000-fold using PBS buffer (10 mM, pH 7.4) and stored at -20°C. For spiked serum samples, GSH standard solution was added to the real samples. The testing procedure for both real and spiked samples was consistent with the previously described protocols for glucose and glutathione.

SERS Measurements

Horiba JY LabRAM HR Evolution Raman spectrometer was used in this paper. A 532 nm laser was employed for excitation with a power of 0.5 mW and a $\times 100$ objective. Spectra were collected for 10 s at each point, with the laser focused on a spot of approximately 4 mm in diameter. The spectrometer was calibrated using the characteristic peak at 520 cm^{-1} of a silicon wafer. MB (10^{-4} M to 10^{-7} M) was used as the Raman probe to assess the SERS activity of the samples.

Calculation of SERS enhancement factor (EF)

We use enhancement factor (EF) to further quantify the SERS performance of substrates by the following equation:

$$EF = \frac{I_{SERS}/N_{SERS}}{I_{RS}/N_{RS}}$$

where I_{SERS} and I_{RS} represent the intensity of SERS spectra and normal Raman spectra, respectively, and N_{SERS} and N_{RS} represent the average number of molecules within the laser spot excited by SERS and normal Raman, respectively. Here, the N_{RS}/N_{SERS} values are estimated from the ratio of the respective molecular concentrations. The minimum detected concentration of VN@C is 10^{-6} M and the peak SERS intensity at 1607 cm^{-1} is 130, while the intensity of 10^{-2} M MB in normal Raman spectra is 467 on the glass slide. $EF = (I_{SERS}/N_{SERS}) / (I_{RS}/N_{RS}) = (130/10^{-6}) / (467/10^{-2}) = 2.8 \times 10^3$. However, the detected concentration of P-VN@C is 10^{-6} M and the SERS peak intensity at 1607 cm^{-1} is 3035, while the intensity of 10^{-2} M MB in normal Raman spectra on the glass slide is 467. So, $EF = (I_{SERS}/N_{SERS}) / (I_{RS}/N_{RS}) = (3035/10^{-6}) / (467/10^{-2}) = 6.5 \times 10^4$

Electronic Structure Computation

All DFT computations were performed using the Vienna ab initio simulation package (VASP). The exchange-correlation interactions were treated with the Perdew-Burke-Ernzerhof (PBE) generalized gradient approximation. A plane-wave basis set with 450 eV kinetic energy cutoff was employed. The Monkhorst-Pack K-points grid was set to $2\pi \times 0.03 \text{ \AA}^{-1}$ and $2\pi \times 0.02 \text{ \AA}^{-1}$ for geometry optimizations and electronic structure calculations, respectively. The convergence criterions of the total energy and residual

Hellmann–Feynman force were set to 10^{-4} eV and 0.02 eV \AA^{-1} for structural optimizations.

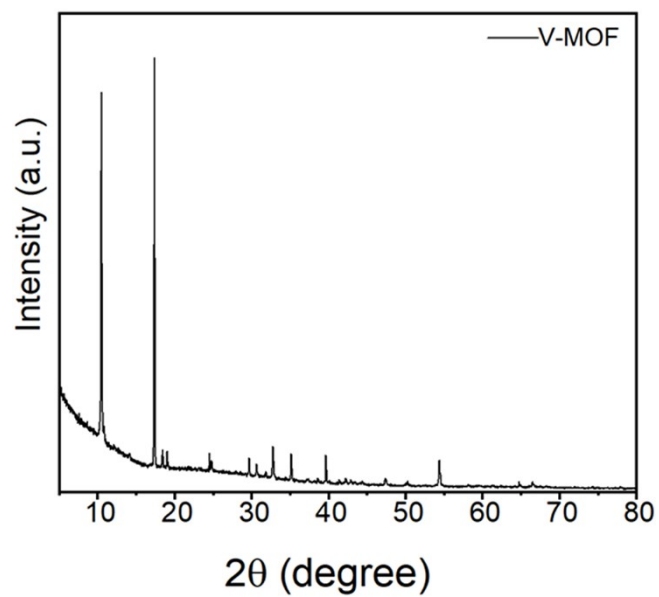


Figure S1. XRD pattern of V-MOF nanowires.

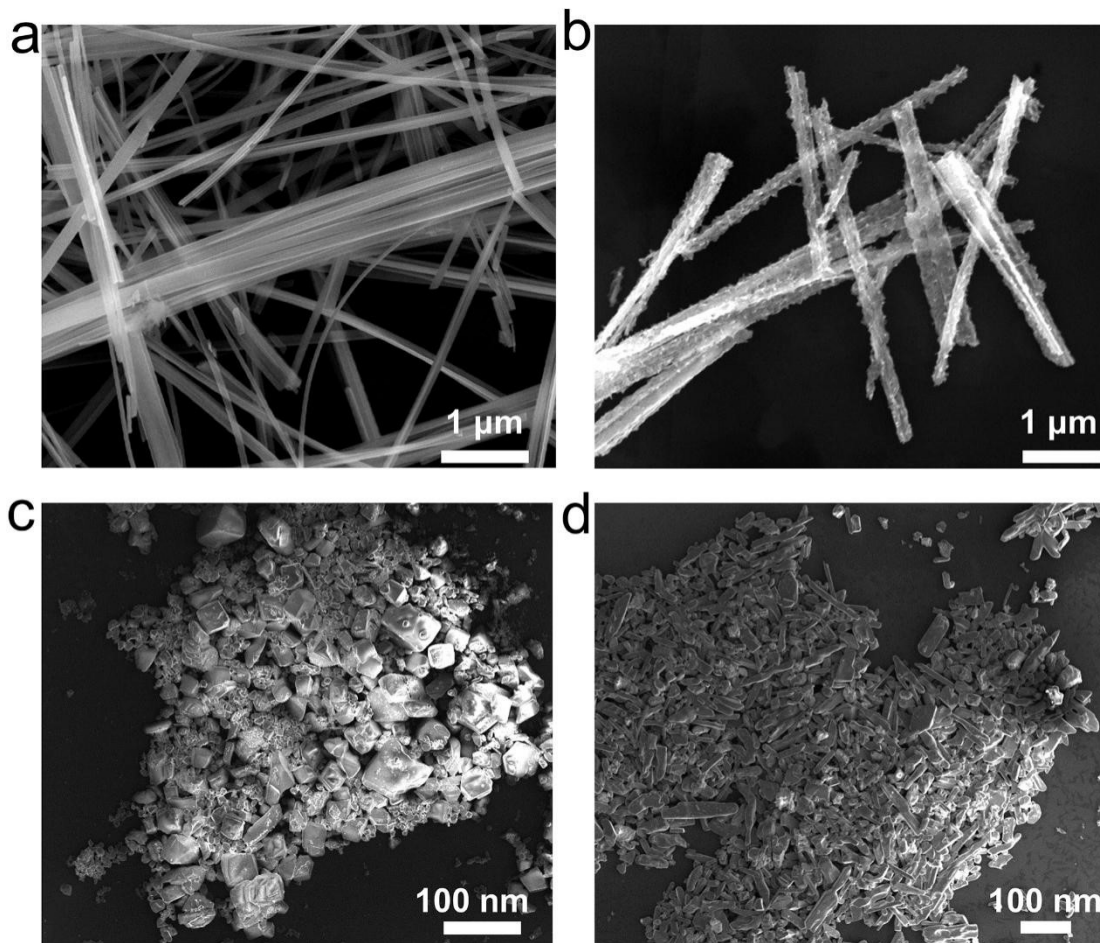


Figure S2. SEM images of VN@C prepared at different temperature. (a) 400 °C; (b) 600 °C; (c) 700 °C; (d) 800 °C.

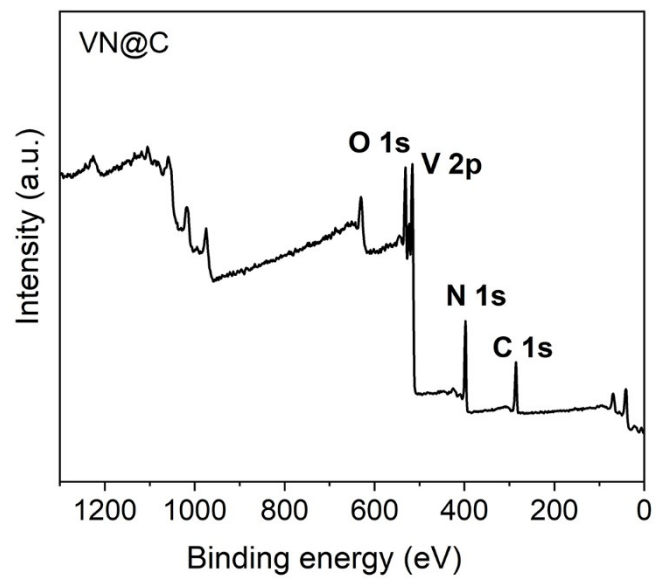


Figure S3. XPS survey spectra of VN@C.

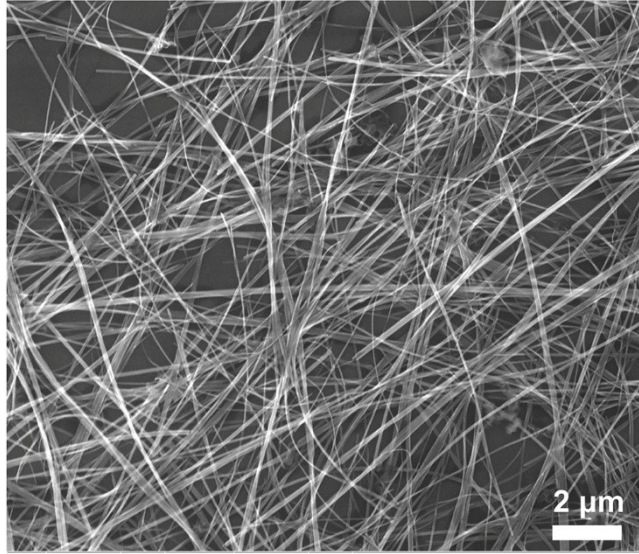


Figure S4. SEM image of VN@C nanowires.

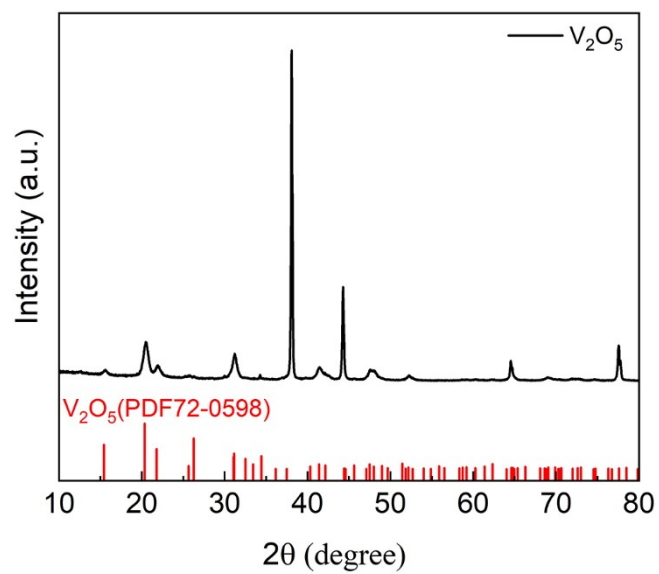


Figure S5. XRD pattern of V₂O₅ nanowires

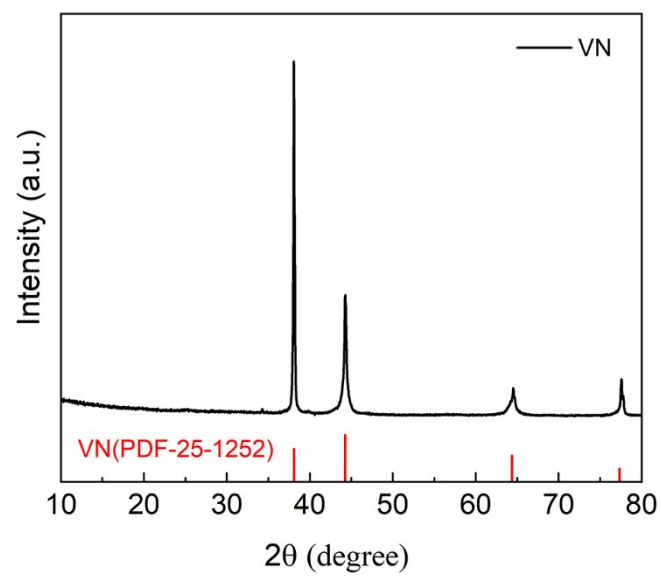


Figure S6. XRD pattern of VN.

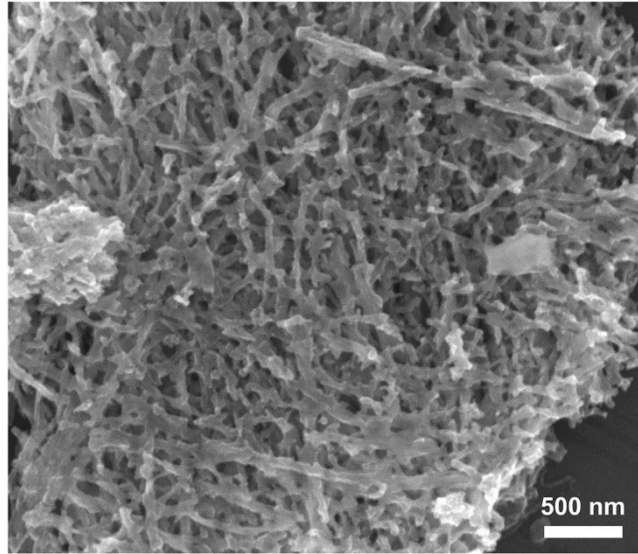


Figure S7. SEM image of VN.

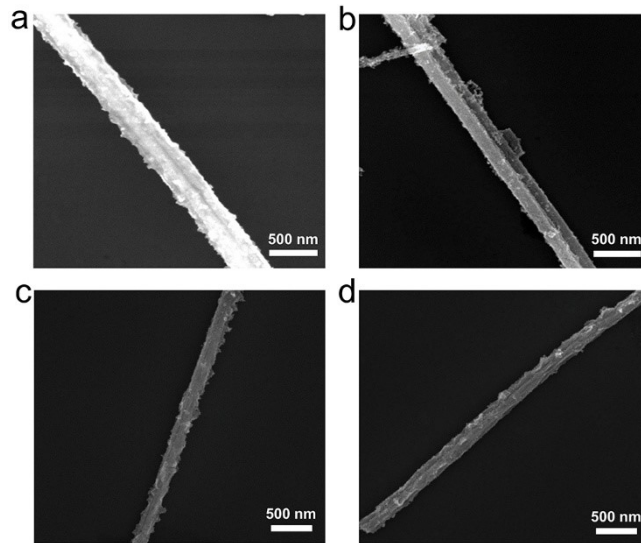


Figure S8. SEM image of P-VN@C generated with NaH_2PO_2 of varying masses. (a) 5 mg, (b) 25 mg, (c) 50 mg, (d) 100 mg.

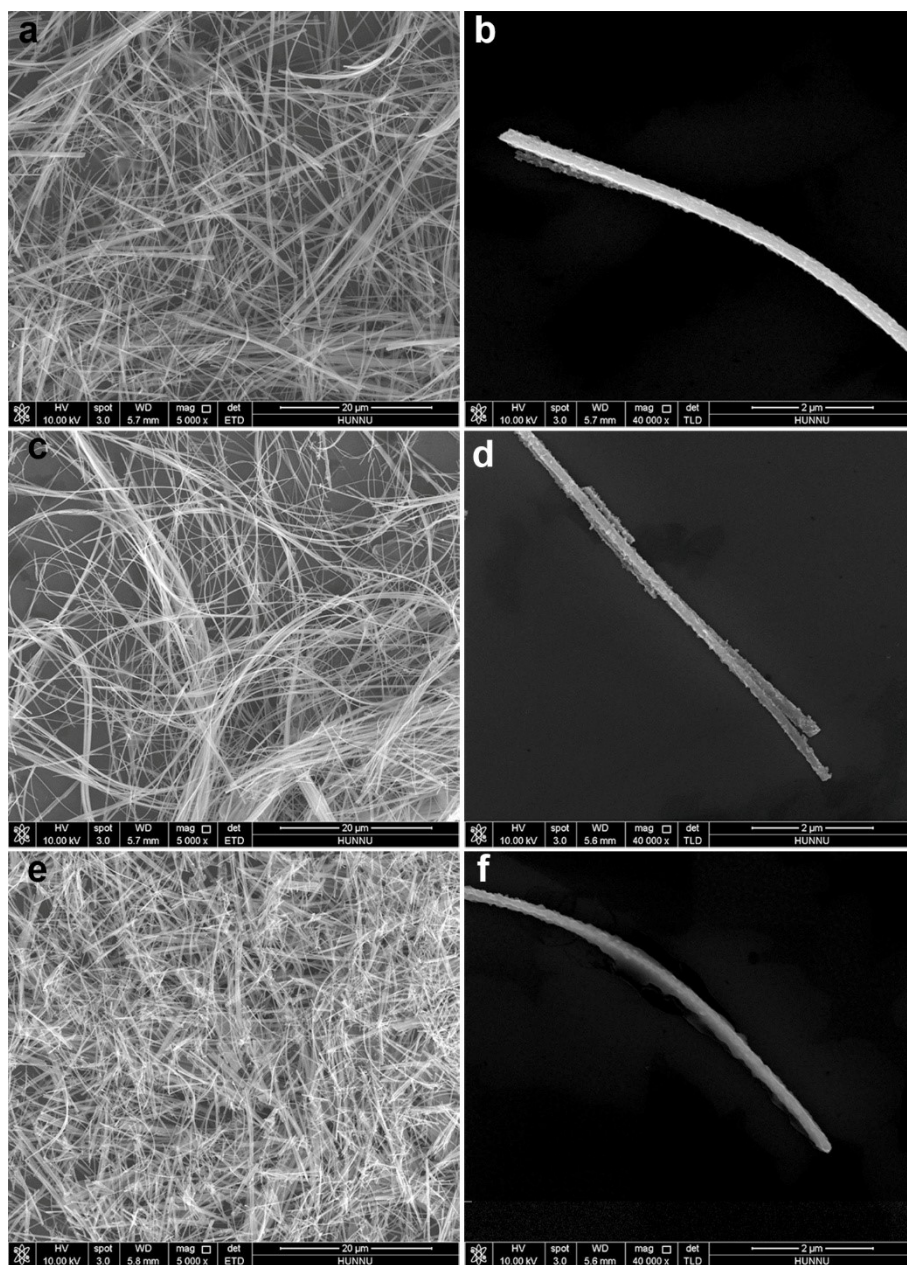


Figure. S9. SEM images of P-VN@C nanowire prepared at different temperature. (a, b) 200°C; (c, d) 300°C; (e, f) 400°C.

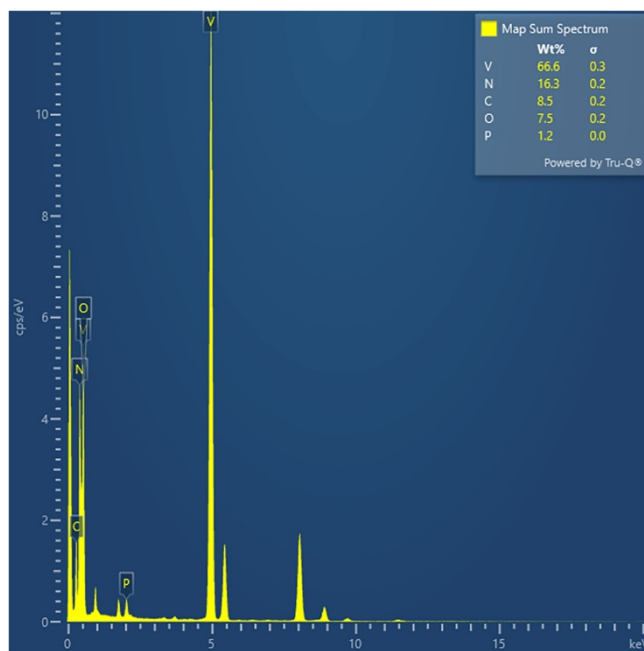


Figure. S10. The EDX spectrum of P-VN@C nanowires.

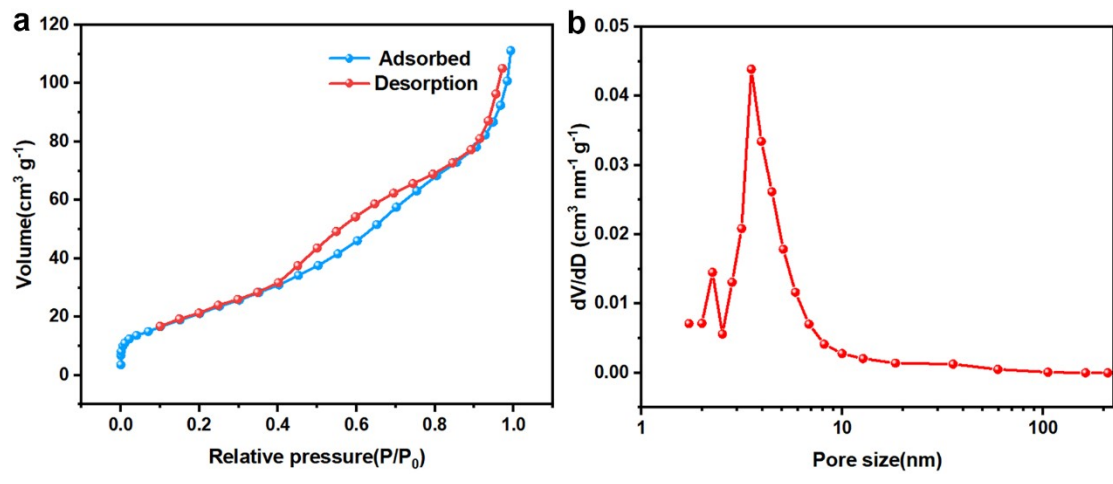


Figure S11. N₂ adsorption-desorption isotherms and the pore-size distribution of P-VN@C.

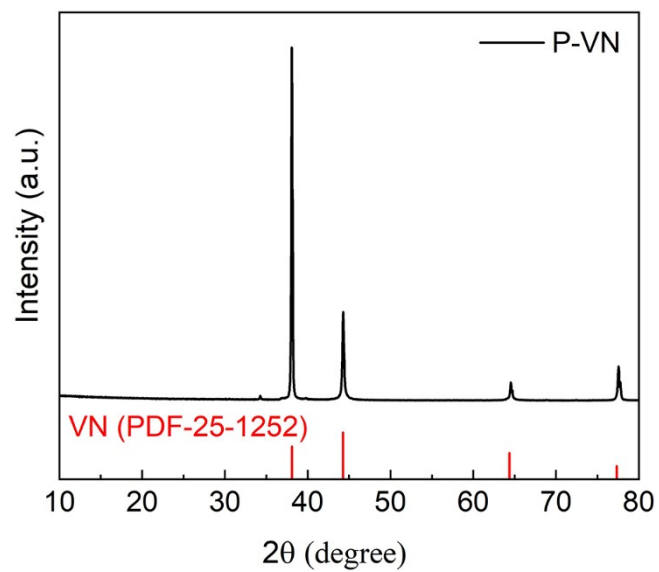


Figure S12. XRD pattern of VN.

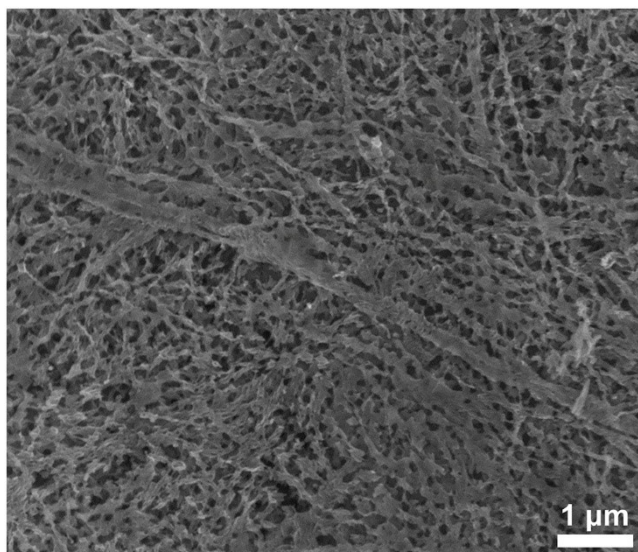


Figure S13. SEM image of P-VN.

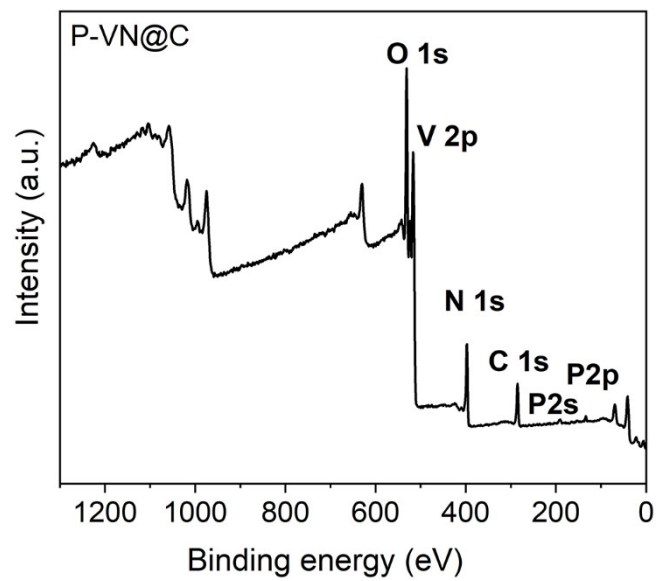


Figure S14. XPS survey spectra of P-VN@C.

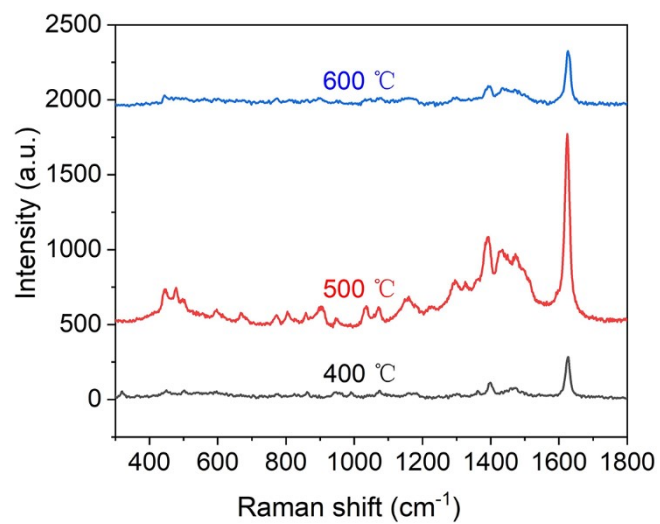


Figure S15. SERS spectra of 10^{-5} M MB detected on VN@C with different reaction temperature.

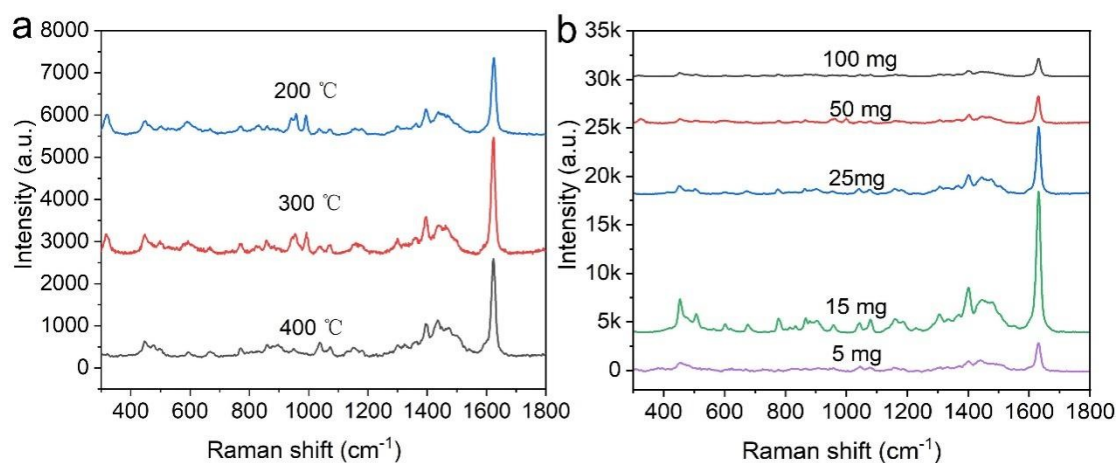


Figure S16. (a) SERS spectra of 10⁻⁵ M MB detected on P-VN@C with different reaction temperature and (b) different NaH₂PO₂ masses.

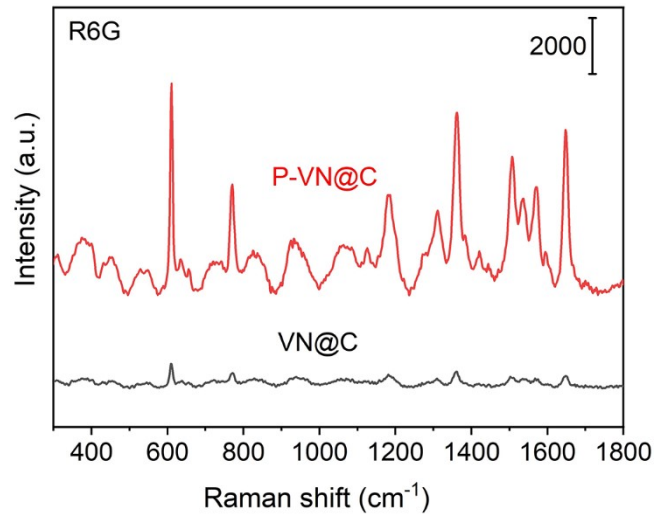


Figure S17. SERS spectra of R6G molecules absorbed on P-VN@C and VN@C.

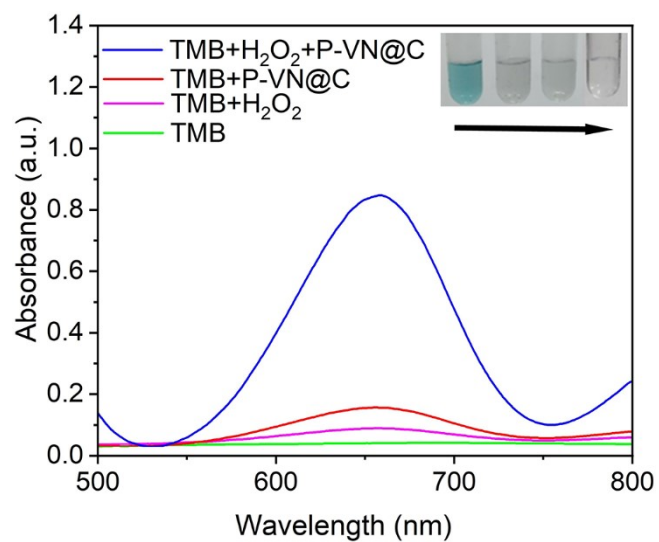


Figure S18. UV-vis spectra for the oxidation reaction of TMB catalyzed by P-VN@C.

The inset shows optical images of the solution color change with increasing GSH concentration.

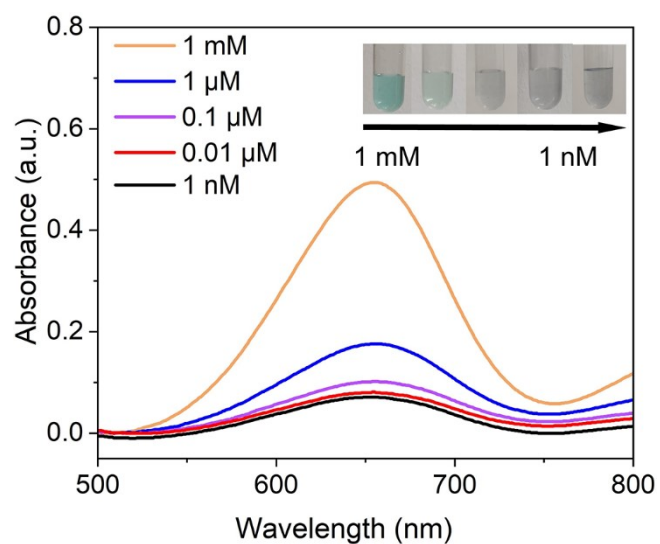


Figure S19. UV-vis spectra for the oxidation reaction of TMB catalyzed by P-VN@C with different concentrations of H₂O₂. The inset shows optical images of the solution color change with increasing H₂O₂ concentration.

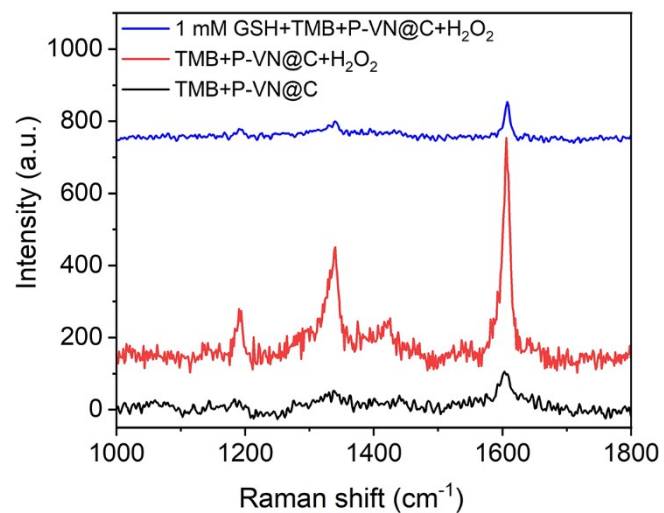


Figure S20. SERS spectra collected on TMB + P-VN@C, and TMB + VN@C + H₂O₂, and 1mM GSH + TMB + VN@C + H₂O₂.

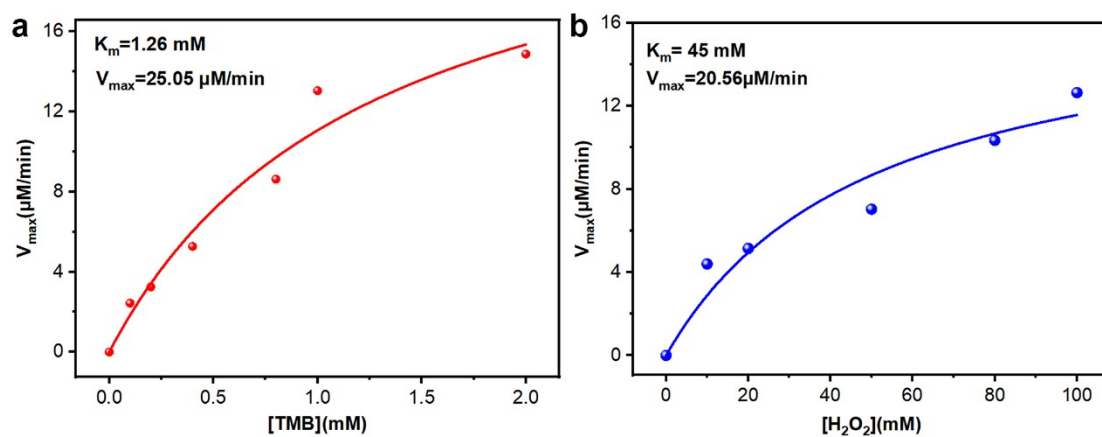


Figure S21. Michaelis–Menten kinetics of P-VN@C nanozymes with (a) varying TMB concentration in 0–2 mM and keeping a H_2O_2 concentration of 10 mM; (c) varying H_2O_2 concentration in 0–100 μM and keeping a TMB concentration of 1 mM.

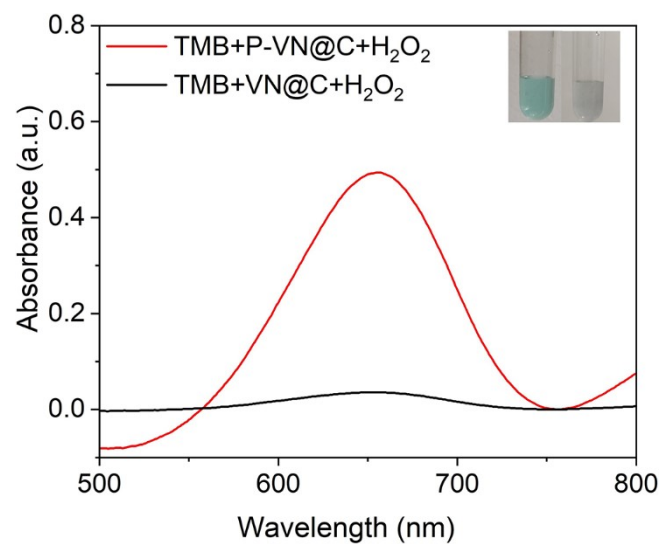


Figure S22. UV-Vis spectra of TMB + P-VN@C + H₂O₂ and TMB + VN@C + H₂O₂.

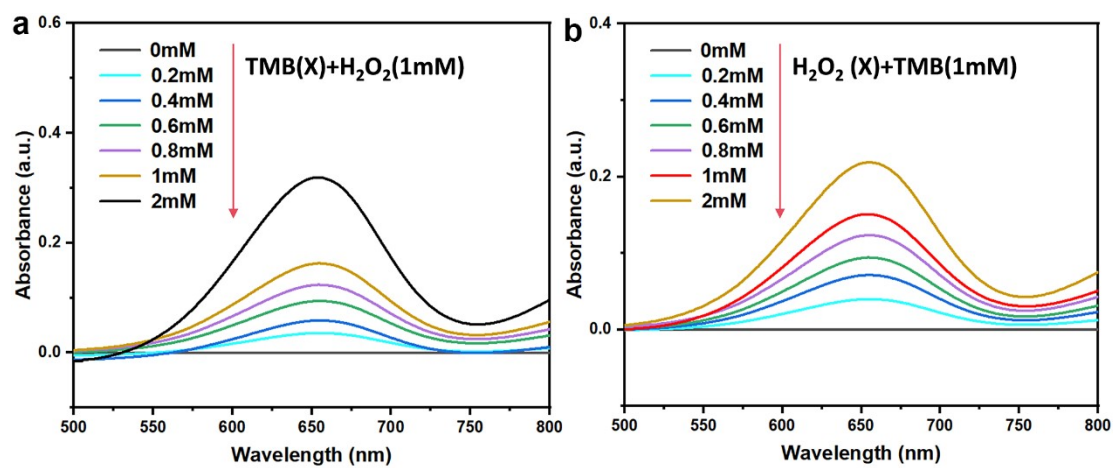


Figure S23. UV-vis spectra collected on (a) P-VN@C + H₂O₂ (1 mM) + TMB (x mM), (b) P-VN@C + H₂O₂ (x mM) + TMB (1 mM).

Table S1 Comparison of GSH performance detected by different methods

Catalyst	Linear Range (μM)	LOD (μM)	Ref.
COF-300-AR	1-15	1	S1
AuVCs	25-500	9.80	S2
CDs@ZIF-8	0-100	1.04	S3
CoOOH	33-1300	13.7	S4
Cu NCs	1-150	0.89	S5
R-Fe ₃ O ₄ /Au	5-200	0.88	S6
NIR fluorescent probe	0-180	6.847	S7
P-VN@C	1-100	1	This work

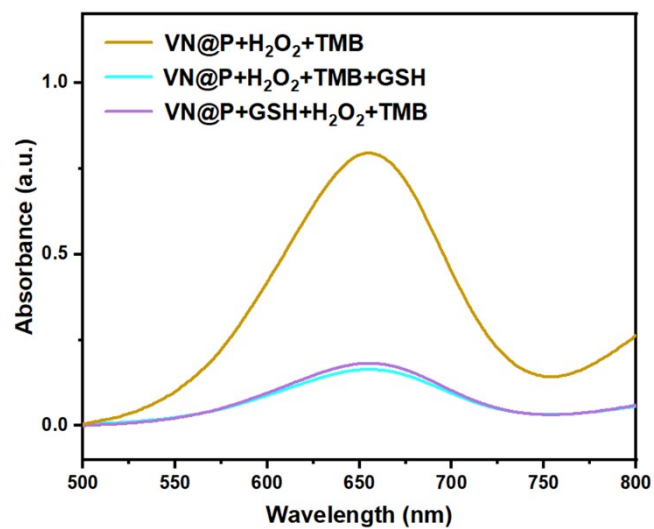


Figure S24. UV-vis spectra collected on P-VN@C + H₂O₂ + TMB, P-VN@C + H₂O₂ + TMB+GSH, P-VN@C +GSH+ H₂O₂ + TMB.

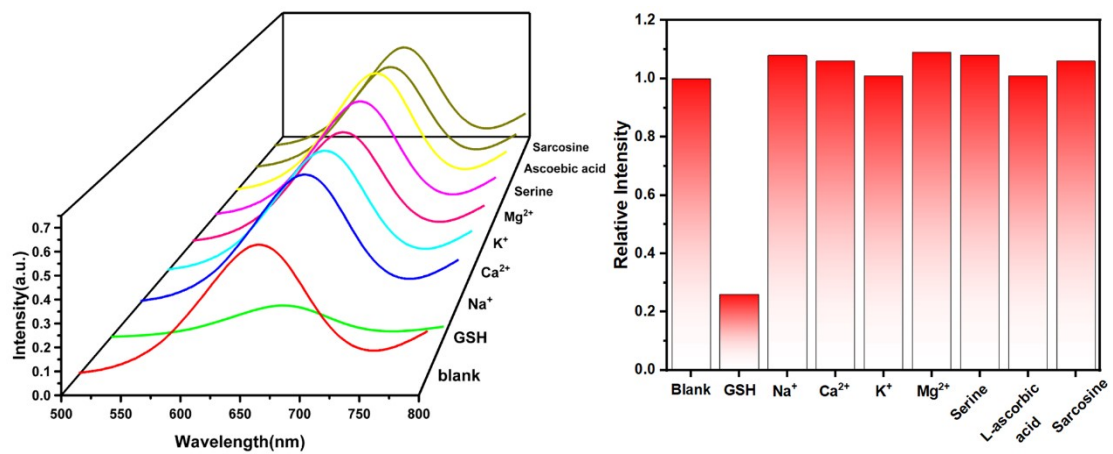


Figure S25. Selectivity of P-VN@C nanowires for GSH detection.

References

1. P. Jin, X. Niu, F. Zhang, K. Dong, H. Dai, H. Zhang, W. Wang, H. Chen and X. Chen. *ACS Appl. Mater. Interfaces*, 2020, **12**, 20414-20422.
2. H. Pang, Y. Ke, N. Li, Y. Chen, C. Huang, K. Wei and H. Yang. *Biosens Bioelectron*, 2020, **165**, 112325.
3. Y. Wang, X. Liu, M. Wang, X. Wang, W. Ma and J. Li. *Sensor Actuat B-Chem*, 2021, **329**, 129115.
4. J. Li, L. Jiao, W. Xu, H. Yan, G. Chen, Y. Wu, L. Hu and W. Gu. *Sensor Actuat B-Chem*, 2021, **329**, 129247.
5. C. Liu, Y. Cai, J. Wang, X. Liu, H. Ren, L. Yan, Y. Zhang, S. Yang, J. Guo and A. Liu. *ACS Appl. Mater. Interfaces*, 2020, **12**, 42521-42530.
6. Y. Huang, Y. Gu, X. Liu, T. Deng, S. Dai, J. Qu, G. Yang and L. Qu. *Biosens Bioelectron*, 2022, **209**, 114253.
7. K. Xiong, F. Huo, J. Chao, Y. Zhang and C. Yin. *Anal. Chem.*, 2018, **91**, 1472–1478.